

SOIL POLYGENESIS AS A FUNCTION OF QUATERNARY CLIMATE CHANGE,
NORTHERN GREAT BASIN, USA

Oliver A. Chadwick, Wiley D. Nettleton, and George J. Staidl

JPL, 183-501, California Institute of Technology, Pasadena CA 91109 (USA)

USDA National Soil Survey Laboratory, Lincoln, NE 68508 (USA)

USDA Soil Conservation Service (retired), Box 972, Pinedale, WY 82941 (USA)

ABSTRACT

The Quaternary environmental history of the northern Great Basin is characterized by a combination of lower temperature and higher moisture than present. Using water-balance analysis of soils sampled along a climatic gradient, we demonstrate that long-term average effective moisture was about 2 - 4 cm yr⁻¹ greater than present. Although this long-term average represents most of Quaternary time, there are important short-term excursions from these values during full glacial and interglacial times. Full glacial conditions are characterized by effective moisture about 7-9 cm yr⁻¹ greater than present; interglacial times, similar to present conditions, are characterized by dry lake basins that provide major increases in eolian activity. These climatic extremes drive pedogenic processes that leave polygenetic imprints on Pleistocene age soils. Soils that are now dominated by opaline silica, carbonate, and smectite contain evidence of earlier, more acidic, chemical environments conducive to dissolution of primary carbonate and formation of kaolinite. During interglacial time, more eolian activity and less effective moisture combine to decrease the depth of leaching, increase base cations, and modify the soil chemical environment in relict paleosols. In a Bull Lake age soil (=150 ky bp), desert loess accumulation created a 25% increase in water holding capacity and decreased the depth of water penetration by 65 cm; climatic drying at the end of the Pleistocene decreased leaching depth by about 150 cm.

INTRODUCTION

Polygenetic soils are those that record multiple morphological, mineralogical, and chemical imprints as the geographical pattern of climates shifts spatially and new boundaries are established (Nikiforoff, 1953). Optimal conditions for interpreting paleoclimates from polygenetic soils occur when precipitation and/or temperature changes are great enough to produce new soil properties without obliterating existing properties. In this classical view, the magnitude of climate shift required for polygenesis is left open, but most investigators consider that polygenesis occurs in response to large changes in climatic patterns such as between glacial and interglacial or interstadial conditions (Nikiforoff, 1953; Bryan and Albritten, 1953; Butler, 1959; McFadden and Tinsley, 1985; Wells et al., 1987; Reheis, 1987; Chadwick and Davis, 1990). Here we document polygenesis in Quaternary soils by separating soil properties inherited during glacial climatic conditions in the Great Basin from those developed in response to the present more arid conditions. Further, to integrate past and present conditions, we simulate changing pedologic environments by sampling along a modern orographically induced climatic gradient.

Today, the northern part of the Basin-and-flange physiographic province is composed of subhumid mountains rising above arid to semiarid basins. Many basins contain dry lake beds that are testaments to earlier climatic conditions when effective moisture was greater (Fig. 1) (Snyder et al., 1964; Hawley and Wilson, 1965; Mifflin and Wheat, 1979; Smith and Street-Perrot, 1983; Benson et al., 1990; Morrison, 1991), Ancient lake shorelines cut mountain slopes, alluvial fans, and glacial deposits of Pleistocene age in many places. Soil profiles on these landforms evolved in the context of changing moisture conditions that control the rates of eolian inputs and mineral weathering through complex interactions among: 1) episodic eolian additions that provide fine-grained silicate and carbonate minerals derived from the dry lake

beds (Peterson, 1980; Nettleton and Peterson, 1983; Wells et al., 1987; Chadwick and Davis, 1990, Reheis, 1990; Harden et al., 1991 b), 2) slow mineral weathering rates when soils are dry for long periods (Locke, 1979; Colman and Pierce, 1981; Hall and Michaud, 1988; Hall and Horn 1993), and 3) changes in the rates and types of pedogenic mineral synthesis - primarily carbonate, gypsum, and smectite during interpluvials and kaolinite and vermiculite during pluvials (Birkeland, 1969; Birkeland and Janda, 1971; Jenny, 1980; Machette, 1985; McFadden and Tinsley, 1985; Harden et al., 1991a; McFadden et al., 1991).

Here, we combine measurements of soil properties with knowledge of present climatic conditions and models of past climatic patterns to understand the effect of environmental change on pedogenesis. First, we document changes in soil chemical, physical, and micromorphical properties as effective moisture changes with increasing elevation in a Great Basin mountain range. Once present-day climate - soil property relationships are established, we use them to interpret polygenetic processes that determine the relict soil properties accumulated during past pluvial climates. We chose to sample glacial till derived from the Ruby Mountains of northeastern Nevada (Fig.1) because it provides a uniformly heterogeneous substrate for soil genesis that covers a large range in elevation and climatic conditions.

MATERIALS AND METHODS

Site description

The Ruby Mountains-East Humboldt Range east of Elko, Nevada lies midway between glacial lakes Lahontan and Bonneville (Fig.1). It is composed of metamorphic rocks of early Paleozoic age (Howard, 1971), mainly quartzites, calcsilicates, and marbles, that have been intruded by granite and granite pegmatite. Rising from piedmont slopes of about 1800 m to crests exceeding 3350 m, it is the most extensively glaciated of the Great Basin mountain ranges. The glacial deposits

sampled in this study issued from the same watershed and are similar to each other in lithology and particle size. They are composed of disintegrated granite, granite gneiss, pegmatite, quartzite, and marble (Wayne, 1984). In their initial state, the deposits had particle sizes ranging from cobbly loamy sand to extremely cobbly loamy sand, Based on microscopic studies of sand grains by Wayne (1984) and ourselves, the parent material is composed of quartz ($62.9 \pm 5.1\%$), K-feldspar ($18.1 \pm 2.6\%$), biotite ($5.3 \pm 2.8\%$), zircon ($3.0 \pm 1.0\%$), calcite ($1.3 \pm 0.5\%$), muscovite ($0.7 \pm 0.5\%$), plagioclase ($0.1 \pm 0.4\%$), and other minerals ($8.4 \pm 4.1\%$) that include hornblende, pyroxene, garnet, and volcanic glass shards.

Glacial deposits and soil ages vary along the transect and for our purposes are separated into two categories: those that have been exposed to at least one full glacial and interglacial climatic cycle and those that have been influenced only by interglacial conditions since their deposition. Four soils (sites 1 - 4; Fig. 2, Tables 1 and 2) were sampled on older Lamoille and pre-Lamoille age deposits that are preserved at lower altitudes. Sites 1 - 4 have been influenced by at least one full glacial - interglacial climate. The exact ages of these deposits are uncertain, but based on landform relationships, sites 1 and 2 are about the same age and older than site 3. Site 3 is correlated to the Bull Lake and Tahoe deposits ($\approx 150,000$ yr bp) of the Rocky Mountain and Sierra Nevada glacial sequences, respectively (Wayne, 1984). Site 4 is younger than site 3, but much older than site 5. Three soils (sites 5- 7; Fig. 2, Tables 1 and 2) were sampled on the younger Angel Lake deposits that are confined to river valleys at higher altitudes and correlated to the Pinedale and Tioga deposits ($\approx 15,000$ yr bp) of the Rocky Mountain and Sierra Nevada sequences, respectively (Wayne, 1984). Sites 5 - 7 have experienced dominantly interglacial climatic condition, As pointed out by Birkeland et al. (1991) erosion of glacial deposits can undermine data interpretation; we sampled on broad moraine crests in areas that have experienced little erosion judging from the exposure of boulders.

Vegetation at Sites 1 -3 is dominated by *Artemesia tridentata wyomingensis* (Wyoming big sage) and bunch grasses (Table 1). At Site 4 *Artemesia arbuscula* (low sagebrush) replaces the Wyoming big sage and at Sites 5 -6 *Artemesia vaseyana* (mountain big sagebrush) replaces the low sagebrush. *Populus tremula tremuloides* (quaking aspen) and bunch grasses dominate at Site 7. Plant species distribution and biomass production (dry weight) were determined by methods outlined in the National Range Handbook (USDA-Soil Conservation Service, 1976),

Climate and soil-water modeling

Climatic data and estimates of effective moisture (Table 2) were derived in the following manner. Mean annual air temperature (MAAT) is estimated for each sample site based on a lapse rate of $0.5^{\circ}\text{C } 100 \text{ m}^{-1}$ (Mifflin and Wheat, 1979; Schmidlin et al., 1983). The initial datum for calculation was 7.0°C at the Lamoille weather station (US Weather Bureau Card Deck) near the base of the transect (Fig. 1). Mean annual precipitation is estimated using a regression equation based on sampling along elevation gradients in the Ruby Mountains (equation [1], USDI-BLM, Nevada State Office, personal communication).

$$\text{MAP (in)} = 0,0048 - 15,66605 (\text{ELEVATION, ft}); r^2 = 0.85 \quad [1]$$

The MAAT and MAP estimates for each site are then apportioned to monthly values based on the monthly proportion of annual precipitation measured at the Lamoille weather station. Monthly precipitation values are combined with potential evapotranspiration derived by the Thornthwaite (1948) method to calculate the water available for leaching using the approach of Mayer (1986) and Mayer et al. (1988). Mean annual soil temperatures (MAST) are calculated using a regression equation based on regional sampling (northeastern Nevada) along elevation gradients (equation 2, Schmidlin et al., 1983).

$$\text{MAST } C = 50.1 - 0.0053 (\text{ELEVATION, ft}) - 0.66 (\text{LATITUDE}); r^2 = 0.72 \quad [2]$$

Assuming that no moisture is lost as surface runoff, we calculated the leaching depth for each soil. Bulk density was measured for about 30% of the horizons; these data were used to calibrate a model that estimates bulk density and water retention at suctions ranging from 0.01 MPa to 1.5 MPa (Baumer, 1991). Inputs to the model are particle size, bulk density, clay activity, organic matter, estimated porosity, and mineralogical composition. The resulting estimates of water retention at 0.03 MPa and 1.5 MPa for the <2-mm fraction are used to calculate water retention difference (WRD) (USDA-Soil Conservation Service, 1992; 4B):

$$\text{WRD} = ((W_{0.03} - W_{1.5})(D_{b0.03}) (C_m)) / 100 \quad [3]$$

Where $W_{0.03}$ and $W_{1.5}$ are water (wt. %) retained at 0.03 and 1.5 MPa, respectively, $D_{b0.03}$ is the bulk density measured at 0.03 MPa, and C_m is the ratio of the moist volume of the <2-mm fabric to the volume of the moist whole soil. WRD is an estimate of available water capacity; it is used to calculate leaching depths and normalize the influence of varying soil textures on properties such as organic carbon and exchange acidity to a common basis.

Soil physical properties affecting water retention were converted to a whole-soil volume percent basis as follows (USDA-Soil Conservation Service, 1992): 1) the 2-5 and 5-20 mm size fractions were determined by weighing sieved fractions from the bulk samples, 2) the >20 mm fraction was estimated in the field, 3) porosity was calculated using the bulk density of the <2 mm fraction and an assumed particle density (2.65 g cm⁻³), and 4) sand, silt, and clay measured on the <2 mm fraction were recalculated taking into account porosity and coarse fragment content. Water retained by the whole soil upon wetting was summed for each horizon to give the depth of leaching (Tables 2 and 3).

Chemical and physical analyses

Soils were analyzed at the National Soil Survey Laboratory (USDA-Soil Conservation Service, 1992): particle-size distribution by sieving and pipette analysis (3A1); water retention at 1.5 MPa using pressure membrane apparatus (462) and at 0.03 MPa using Saran coated clods (4A1) and pressure plate apparatus (4B1); organic carbon by acid bichromate digestion and FeSO_4 titration (6A1); base cations by ammonium acetate extraction at pH 7 (5 B5a); exchangeable acidity by BaCl_2 triethanolamine extraction buffered at pH 8.2 (6 H5a); pH measured in a 0.01 M CaCl_2 1:2 soil water solution (8 Cl f); calcium carbonate by manometer measurement of CO_2 evolved following HCl treatment (6E1 b); base saturation by sum of cations method, pH 8.2 (5C3); and clay mineralogy by X-ray diffraction (7A2i) and differential thermal analysis (7A6). Thin sections were prepared commercially and observed for related distribution patterns of coarse and fine constituents (Stoops and Jongerius, 1975; Bullock, et al., 1985) and plasmic fabrics (Brewer 19-/6).

The glacial parent material is dominated by coarse fragments and loamy sand fine-earth fraction, but over time it has trapped eolian dust. For a quantitative analysis of eolian input to selected transect soils, we assume that all silt and clay in the A and B horizons that is greater than that in the glacial parent material are either introduced from atmospheric sources or formed by weathering. Analysis of desert loess deposits in northern Nevada indicate that the ratio of clay to silt in the regional loess is about 0.2. We apply this ratio to the accumulation of silt and clay to determine the amount of eolian clay and attribute the excess to pedologic clay mineral formation. This analysis includes weathering of eolian silt and sand-size minerals in the parent material. Estimates of eolian input to the soils are minimum values; we use silt as an index and a portion of the silt has weathered to clay. Quantitative analysis of loess accumulation and clay formation is applied to soil profiles sampled at sites 3, 5, and 6 because we are most certain about parent material properties and age at these sites.

RESULTS

Soil genesis in the glacial deposits along the transect are subject to the following cascade of natural processes: 1) effective moisture determined by the interaction of climate and soil water-holding properties, 2) biomass as a function of effective moisture, 3) organic carbon as a function of biomass, 4) base saturation and exchange acidity as a function of organic carbon, and 5) mineral species as a function of base saturation, exchange acidity, and eolian additions. Below we characterize the specific features of each level determining soil properties along the transect.

Effective moisture and depth of leaching

Effective moisture increases with increasing elevation (Table 2) due to orographic precipitation and the temperature lapse that lowers potential evapotranspiration (Houghton et al., 1975). Average annual effective moisture is about 14, 15 and 16 cm, for sites 1, 2, and 3 respectively (Table 2). When combined with WRD values (Table 3), maximum depths of leaching are predicted at about 100, 125, and 200 cm respectively (Table 2). Average annual effective moisture at site 4 is about 17 cm; predicted wetting depth is about 325 cm (based on extending the water retention for the deepest horizon). With increasing elevation along the transect, site 4 is the first soil with no carbonate and pH below 7 (Table 4). Average annual effective moisture is about 22, 27, and 37 cm for sites 5, 6, and 7, respectively. The predicted depth of leaching is about 550, 400, and 650 cm, respectively.

Compared to CaCO_3 distribution, the predicted wetting depths appear too great (Table 4). Assuming that CaCO_3 precipitates near the maximum depth of wetting, site 1 shows CaCO_3 from 63 to >90 cm, site 2 has CaCO_3 from 62 to 125 cm, and site 3 has CaCO_3 from 86 to 150 cm. Porosity discontinuities at 63, 95, and 86 cm for sites 1, 2, and 3 respectively (Table 3) may have truncated depth of wetting and carbonate

precipitation. In addition, some of the difference between predicted wetting depth and observed carbonate distribution is due to unaccounted surface runoff.

Biomass, organic carbon, and exchange properties

Biomass production increased with increasing elevation and precipitation with two exceptions (Tables 1 and 2). Site 2 has higher production than sites 3 and 4, because it has been seeded to a near monoculture of crested wheatgrass (*Agropyron cristatum*). Site 7 has less production than site 6 because the negative effects of low temperature and short growing season overwhelm any plant growth enhancement by greater moisture.

Organic carbon and exchange acidity increase and base saturation and pH decrease as effective moisture (EM) increases along the transect (Fig. 3, Table 4). Increasing effective moisture along the transect is responsible for soil classifications that range from Aridisols and Xerolls to Cryoborolls and Cryumbrepts. For organic carbon (OC), the measured values along the transect are described by the following relationship: $[OC = 0.70(EM) - 1.32(EM)^2 - 6.63]$; $r^2 = 0.94$. Change in soil organic carbon follows the pattern for estimated biomass production suggesting that the decrease in organic carbon at site 7 is related to lower biomass production (Table 1). In contrast, exchange acidity (EA) increases with elevation all along the transect, though the rate of change decreases at high elevation (Fig. 3) as described by the following relationship: $[EA = 15.82(EM) - 0.25(EM)^2 - 162.73]$; $r^2 = 0.90$. The amount of exchange acidity is controlled by inputs of organic acids that stimulate mass action replacement of bases by aluminum on the exchange complex during leaching (Tan, 1992, pp. 307-308). At site 7, exchange acidity does not drop relative to site 6 because although biomass production and organic carbon have decreased, leaching intensity has increased. Thus, the level of exchange acidity represents a balance between biomass production and leaching. In response to increasing acidity, base saturation

(BS) decreases linearly with increasing elevation (Fig. 3) as described by the following relationship: $[BS = 141.38 - 3.02(EM)]$; $r^2 = 0.98$. Not surprisingly, pt-f decreases from between 7 and 8 at sites 1-3 to near 5 at site 7 (Table 4). Overall acidification of the soil exchange complex with increasing effective moisture implies differences in the clay mineral species that are synthesized from mineral weathering products.

Occurrence *and* ^l~~d~~istribution of soil minerals

The glacially derived parent material has a small clay-size fraction that includes about 230 ± 30 g kg⁻¹ mica (the average mica content of the clay fractions of C horizons at sites 4 and 6, assuming that clay mica contains 10% of K₂O; Table 4). Sand-size biotites are few in number in sites 1-3 and more common in sites 4-7 (Table 5). Ends of the grains are frayed and partly expanded with loss of pleochroism indicating that the surviving grain fabrics are weathering to vermiculite. The Hornblende and pyroxene are weathered along cleavage traces at sites 1-5, but are only slightly weathered at sites 6 and 7. Plagioclase is pitted and somewhat weathered along cleavage traces at sites 1-4 and only slightly weathered at sites 5-7. Sand-size and larger calcite grains derived from marble are rare; they probably weathered away already.

The argillic horizons in sites 1-4 have fewer coarse fragments compared with the underlying glacial deposit, implying that the fines are derived from eolian sources (McFadden et al., 1987; Chadwick and Davis, 1990). Clay skins described for the argillic horizons in sites 1-4 are stress cutans (Fig. 4B; Table 5), but these soils have A and C horizons with true illuviation argillans on and bridging between sand grains (Fig. 4A). Although, sites 5-7 do not have the measured clay increase indicative of argillic horizons, they do have illuviation argillans on and bridging between sand grains (Table 5). The illuvial silt and clay in soils at sites 5-7 are probably derived from eolian sources because there is little silt and clay in the parent material.

Accumulation of eolian silt in the sola of soils at sites 1-4 ranges from 0.6 to 1.0 kg cm⁻² and silt + clay accumulation ranges from 1.9 to 7.4 kg cm⁻². Weathering of the soil profile at site 3, created about 2 kg cm⁻² clay-size minerals (Table 6). Accumulation of eolian silt in the sola of the soils at sites 5 and 6 is 0.2 and 0.4 kg cm⁻², respectively, and silt + clay accumulation is 0.7 kg cm⁻² for both soils. Weathering of the soil profiles at sites 5 and 6 created about 0.15 and 0.35 kg cm⁻², clay-size minerals, respectively (Table 6). Silt accumulation in the sola of the soil at site 7 is 1.4 kg cm⁻² and silt + clay accumulation is 2.0 kg cm⁻². The mineralogy of the silt fraction of the unweathered loess is dominated by quartz and feldspar with smaller amounts of chlorite; the clay fraction is composed of mica with smaller amounts of smectite and chlorite. Kaolinite occurs in trace amounts only.

Opaline silica and carbonate precipitated in the soil sola are indicators of low effective moisture (Chadwick et al., 1987). Sites 1 - 3 contain enough pedogenic carbonate to meet the criteria for calcic horizons (Table 4), the first two, however, are more cemented by opaline silica than by carbonate. In these pedons, opaline silica and carbonate coat some skeleton grains, but more commonly, they partially coat illuviation argillans in voids and channels or occur as silt-size nodules and concretions within the matrix of deeper horizons (Fig. 5; Table 5). The silans, calcans, nodules and concretions are pedogenic features that accumulated after the argillans. Sites 4- 7 have argillans but lack carbonate or opaline silica. Along the transect, a distinct threshold in opaline silica and carbonate precipitation is reached between sites 3 and 4; sites 4-7 lack opaline silica or carbonate. The effective moisture is 16 cm and 17 cm for sites 3 and 4, respectively (Table 2), but the predicted depth of leaching is 200 cm and 325 cm, respectively. The dramatic difference in leaching depth occurs because site 4 is younger than site 3 and has accumulated less eolian fines (Table 3).

Smectite forms in a chemical environment with relatively high H₄SiO₄ and exchangeable base concentrations (Kittrick, 1969). In well drained soils, its presence

indicates weak leaching intensity. Smectite dominates the B horizon clay fractions of soils at sites 1-3 and is an important mineral at site 4 (Fig. 6), but no smectite was detected in the B horizons at sites 5-7. The relationship among cation exchange capacity (CEC), clay, and organic carbon (OC) at sites 1-3 [$CE:C_{NH_4OAC} = 0.95(\text{clay}) + 2.54(\text{OC}) - 4.4$]; $n = 21$, $r^2 = 0.85$, standard error of regression coefficient of clay = 0.09] is common for smectites formed in arid soils (Nettleton and Brasher, 1983). Lack of smectite at sites 5-7 demonstrates that the chemical status of these soils is not conducive to smectite synthesis and the amount of smectite inherited for desert loess is below detection using standard X-ray diffraction techniques.

Kaolinite forms in chemical environments with relatively high exchange acidity and low H_4SiO_4 and exchangeable bases (Kittrick, 1969). It is present in trace to moderate amounts in the B horizons of all soils (Fig. 6), but under present climatic conditions it is probably only forming in the soils at sites 5-7 because of their lower base saturation and pH (Table 4). Kaolinite in soils 1-3 either formed during wetter climatic conditions or was inherited from eolian dust. Evidence that it formed early in the development of the soils at sites 1-3 can be derived from observations that leaching was intense enough to remove primary calcite from the sola even though pedogenic carbonate is now present in the soils (Tables 4 and 5). Clay illuviation that was prominent early in profile genesis at site 2 has been replaced by illuviation of opaline silica and carbonate (Fig. 4A). Desert loess contains little kaolinite suggesting that the kaolinite was authigenic.

Mica minerals in the B horizons (Fig. 6) are derived from different sources along the transect. Based on microscopic observations (Table 5), the mica is an illitic weathering product at sites 1-4 and physically ground biotite, muscovite, and sericite at sites 5-7. Estimates of clay mica derived from the K_2O content of the $< 2 \mu m$ fraction (assuming that clay mica contains 3.4% K (Nelson and Nettleton, 1975)) range from 200-800 g kg⁻¹ with the greatest amounts in sites 1-4. Thus, it is inappropriate to

use a K value of 3.4% for sites 5-7 because primary mica has K values of about 10% (Jackson and Mackenzie, 1964). Recalculated on this primary mineral basis sites 5-7 have mica contents of about 200 g kg⁻¹, suggesting no significant change from the parent material. Much of the illite at sites 1 -4 is derived from weathering of desert loess.

DISCUSSION

The soils at sites 1 -4 are polygenetic; their characteristics developed during one or more pluvial climates as well as interpluvial climates. On the other hand, the soils at sites 5 - 7 are influenced solely by Holocene climatic conditions that were relatively similar to present conditions (Thompson, 1992). Soil properties that come into relatively rapid equilibrium with new climatic conditions can be interpreted with direct reference to the climatic transect. I-bus, organic carbon concentration, base saturation and extractable acidity on the soil exchange complex, and presence and/or depth distribution of opaline silica and calcium carbonate are dependent on present climatic conditions. In contrast, mineral weathering, the amount of silicate clay, and its mineral composition are dependent on both past and present climates and must be interpreted with reference to: 1) the present distribution of soil properties along a climatic gradient, 2) soil properties that are out of equilibrium with present climatic and pedologic conditions, 3) the sequence of soil mineral deposition based on observation of cross cutting relationships, and 4) nature of past climatic change.

At the dry end on the transect, base saturation above 80%, alkaline pH, and an ample supply of H₄SiO₄ (presence of amorphous silica) favors formation of smectite over kaolinite (Kittrick, 1969). Lower base saturation and H₄SiO₄ at sites 5-7 favors formation of kaolinite over smectite. Apparently, the kaolinite in soils at sites 1 -4

formed during wetter paleoclimates because superpositioning of silans and calcans over argillans indicates a decrease in effective moisture (Reheis, 1987).

The role of desert loess is critical to understanding climatically controlled soil processes in this region. Loess accumulation is episodic; it is more rapid during interpluvial periods when lake basins are bare and subject of periodic deflation (Harden et al., 1991 b; Chadwick and Davis, 1990; Harden, 1990, Reheis et al., 1989). Along the transect the soils forming in Angel Lake deposits accumulate loess at about twice the rate of the soils forming in the Lamoille deposits (Table 6). A major source of desert loess is the Lahontan hydrologic basin composed of the Humboldt River floodplain and playas in a number of closed basins that were connected to form pluvial lake Lahontan (Fig. 1). In addition, the sites probably also received loess from local outwash deposits near the mouth of Lamoille canyon. For comparison, the soil at site 3 has accumulated silt + clay at a rate that is about 7 % of the input to similar age Eetza shorelines and soils at sites 5 and 6 accumulated silt + clay at a rate that is about 10 % of the input to similar age Sehoos shorelines on the east side of the Lahontan playa (Carson Desert area) which is one of the dominant source areas of desert loess in the northern Great Basin region (Chadwick and Davis, 1990).

The climatically controlled pulses of loess introduce fines into the coarse grained glacial sediment. The resulting soil profiles have greater surface area which serves to increase water retention and mineral weathering, and decrease the depth of leaching. Site 3 for example, has a parent material WRD of 0.06 cm cm^{-1} (Table 3), but since deposition, it has received about 3.8 kg cm^{-2} silt + clay as desert loess (Table 6) which is responsible for an increase in water held at field capacity of 3.8 cm ($\approx 25 \%$) (calculated using data in Table 3). If precipitation remained constant during profile development at site 3, the depth of leaching would be decreased by about 65 cm by the accumulation of desert loess. In Holocene time, climatic drying has combined with

the increase in WRD to greatly reduce leaching depth in the transect soils, as discussed below.

During the Pleistocene, the orographically derived climatic gradient interacted with Great Basin topography in the same overall configuration, but most of the landscape had greater effective moisture produced by increased precipitation and lower temperatures (Hawley and Wilson, 1965; Thompson and Mead, 1982). Based on a detailed study of the paleohydrology of pluvial lakes in Nevada, Mifflin and Wheat, (1979) estimate that a 3 °C mean annual temperature decrease and a corresponding 68% increase in precipitation would produce sufficient effective moisture to support the lakes that prevailed about 15,000 years ago. Applying these estimates to our transect indicates that at full glacial time, the soils at sites 1-3 were influenced by 7-9 cm yr⁻¹ greater effective moisture than today which is similar to the present effective moisture conditions at sites 5 and 6 (Table 2), For the soil at site 3, leaching depth was 150 cm greater than present. In summary, the desert loess accumulation decreased water penetration by 65 cm over a period of about 150,000 years and climatic drying at the end of the Pleistocene decreased leaching depth by about 150 cm.

Today, soils at sites 1-3 have chemical conditions conducive to formation of opaline silica, carbonate, and smectite, but judging from the chemical conditions prevalent at sites 5 and 6, kaolinite formed in the past. In this scenario, interpluvial eolian processes would act to recharge the base cations and introduce silica sources (tephra) necessary to transform the chemistry of sites 1-3 to their present state which favors opaline silica, carbonate, and smectite formation (Chadwick et al., 1989). Even though these soils classify as Aridisols today, they would have classified as Alfisols during full glacial periods.

Properties of the polygenetic soils at the dry end of the transect represent the cumulative effect of climatic conditions that fall between those at present and those modeled for full glacial periods (Porter, 1989; Thompson, 1992). The dominance of smectite in the soils of sites 1 -3 suggests that for much of their history these soils were influenced by climatic conditions with less effective moisture than exists at sites 5 and 6 today. The soils at sites 4 and 5 provide an indication of this intermediate effective moisture condition because they bracket the transition to soils with no smectite. The soil at site 4 contains relatively similar amounts of smectite and kaolinite. It has present-day effective moisture of about 17.2 cm yr⁻¹. The soil at site 5 contains no smectite and has an effective moisture of 22.4 cm yr⁻¹. Assuming that the transition occurred closer to site 4 than site 5, the long-term average effective moisture regime for sites 1 -3 was not much greater than about 18 cm yr⁻¹ or about 2-4 cm yr⁻¹ greater than the present values at sites 1 -3. These sites probably supported more *Festuca idahoensis* and *Artemisia vaseyana* and less *Poa secunda*, *Artemisia tridentata*, and *Artemisia arbuscula*.

CONCLUSIONS

An elevation transect in glacial deposits derived from a common source provides a substrate for quantifying the pedogenic effect of present-day and past changes in effective moisture. With increasing elevation, precipitation increases and temperature decreases with resultant effective moisture that increases from 14 to 37 cm yr⁻¹. In the low elevation soils, annual moisture infiltrates to 1 - 2 m, whereas at higher elevations, soils are leached to as much as 5 m depth. Organic carbon increases along the transect except at the highest site where the short growing season depresses biomass production. Driven by increased leaching and accumulation of organic acids, exchange acidity increases and base saturation decreases along the transect. Opaline silica, carbonate, and smectite dominate the pedogenic minerals in

soils with effective moisture $< 16 \text{ cm yr}^{-1}$ and kaolinite is the main pedogenic mineral in soils with effective moisture of $> 22 \text{ cm yr}^{-1}$. Since the glacial deposits vary in age, interpretations regarding the effect of climatic conditions on mineral weathering, clay content, and mineralogy must take polygenesis into account. Relict soils at low elevation sites that now have $14 - 16 \text{ cm yr}^{-1}$ effective moisture and a chemical environment favoring smectite mineral synthesis, probably had about $7 - 9 \text{ cm yr}^{-1}$ greater effective moisture at full glacial time and a chemical environment favoring kaolinite mineral synthesis. At the ^{dryer} sites when both pluvial and interpluvial time is considered, long-term average effective moisture was about $2-4 \text{ cm yr}^{-1}$ greater than present.

Pleistocene soils in the Great Basin record paleoenvironments different from present. The paleoenvironmental changes documented for the dry soils on the Ruby Mountain piedmont influenced the entire Great Basin region. The lower elevation basins (1 200- 1400 m) associated with Lakes Lahontan and Bonneville have lower effective moisture today than sites 1 - 3 (Houghton et al., 1975). The soils contain greater amounts of salts and carbonates, support desert scrub species such as *Atriplex* spp. and have less organic carbon (Thompson and Mead, 1982). Our evidence suggests that Pleistocene piedmont soils in these lower elevation regions had a similar increase in long-term average effective moisture that leached salts, supported *Artemisia tridentata*, and sequestered more carbon. Clearly, in arid and semiarid environments, small changes in effective moisture trigger important changes in soil-ecosystem functioning.

ACKNOWLEDGEMENTS

We are indebted to many researchers with interests in the Great Basin for field discussions and comments on earlier versions of this paper, among them are: Alan Gillespie, Fred Peterson, Peter Birkeland, Bill Wayne, Eugene Kelly, Ted Elliott, Jennifer Harden, Bill Dollarhide, Marith Reheis, Les McFadden, Eric McDonald, Otto Baumer, Ronald Amundson, Janis Boettinger, and Jonathan Davis (lost but not forgotten). Research supported by the University of Washington and the Jet Propulsion Laboratory, California Institute of Technology, both under contract with NASA, and the USDA National Soil Survey Laboratory.

REFERENCES

- Baumer, O. W., 1991. Prediction of soil hydraulic parameters. In: U. S.D.A. Agricultural Research Service Soil Salinity Laboratory, Editor, Indirect Methods for Estimating the Hydraulic Properties of Unsaturated Soils,
- Benson, L. V., Currey, D. R., Dorn, R. I., Lajoie, K. R., Oviatt, C. G., Robins, S. W., Smith, G. I., and Stine, S., 1990. Chronology of expansion and contraction of four Great Basin lake systems during the past 35,000 years. *Paleogeography, Paleoclimatology, and Paleoecology*, 78:241-286.
- Birkeland, P. W., 1969. Quarternary paleoclimatic implications of soil clay mineral distribution in a Sierra Nevada-Great Basin transect. *J. Geology*, 77:289-302.
- Birkeland, P. W., 1984. *Soils and Geomorphology*. Oxford University Press, New York. 372 pp.
- Birkeland, P. W., and Janda, R. J., 1971. Clay mineralogy of soils developed from Quaternary deposits of the eastern Sierra Nevada, California. *Geol. Soc. Amer. Bull.*, 82:2495-2514.
- Birkeland, P. W., Berry, M. E., and Swanson, D. K., 1991. Use of soil catena data for estimating relative ages of moraines. *Geology*, 19:281-283.
- Brewer, R., 1976. *Fabric and mineral analysis of soil*. R.E. Kriger Publishing Co., New York, 482 pp.
- Bryan, K, and Albritton, Jr., C. C., 1953. Soil phenomena as evidence of climatic changes. *Am. Jour. Sci.*, 241:469-490.

- Bullock, P., Fedoroff N., Jongerius, A., Stoops, G., Tursina, T., and Babel, U., 1985. Handbook for soil thin section description. Wayne Research Publications, Wolverhampton, England, 152 pp.
- Butler, B. E., 1959. Periodic phenomena in landscapes as a basis for soil studies. CSIRO, Australia, Soil Publication No. 14.
- Chadwick, O. A., and Davis, J. O., 1990. Soil-forming intervals caused by eolian sediment pulses in the Lahontan Basin, northwestern Nevada. *Geology*, 18: 243-246.
- Chadwick, O. A., Hendricks, D. M., and Nettleton, W.D., 1989. Silicification of Holocene soils in northern Monitor Valley, Nevada. *Soil Sci. Soc. Am. J.*, 53:158-164.
- Chadwick, O. A., Hendricks, D. M., and Nettleton, W. D., 1987. Silica in duric soils: 1. A depositional model. *Soil Sci. Soc. Am. J.*, 51:975-982.
- Colman, S.M. and Pierce, K. L., 1981. Weathering rinds on andesitic and basaltic stones as a Quaternary age indicator, western United States. U.S. Geological Survey Professional Paper 1210, 56p.
- Hall, R.D. and Horn, L. L., 1993. Rates of hornblende etching in soils in glacial deposits of the northern Rocky Mountains (Wyoming-Montana, USA): Influence of climate and characteristics of the parent material. *Chemical Geology*, 105:17-29.
- Hall, R.D. and Michaud, D., 1988. The use hornblende etching, clast weathering, and soils to date alpine glacial and periglacial deposits: A study from southwestern Montana. *Geol. Soc. Am. Bull.*, 100:458-467.
- Harden, J. W., 1990. Soil development on stable landforms and implications for landscape studies. *Geomorphology*, 3:391-398.

- Harden, J. W., Taylor, E. M., McFadden, L. D., and Reheis, M. C., 1991a. Calcic, gypsic, and siliceous soil chronosequences in arid and semiarid environments, pp. 1 - 16. IN: W.D. Nettleton, Editor, Occurrence, Characteristics, and Genesis of Carbonate, Gypsum, and Silica Accumulations in Soils. SSSA Special Paper No. 26.
- Harden, J. W., Taylor, E.M, Hill, C., Mark, R. K., McFadden, L. D., Reheis, M. C., Sowers, J. M., and Wells, S. G., 1991 b. Rates of soil development from four soil chronosequences in the southern Great Basin. *Quaternary Research*, 35:383-399.
- Hawley, J. W., and Wilson, W. E., 1965. Quaternary Geology of the Winnemucca Area, Nevada. Desert Research Inst., University of Nevada, Reno. Tech. Report No. 5.
- Houghton, J. G., Sakamoto, C. M., and Gifford, R.O., 1975. Nevada's Weather and Climate. Nevada Bureau of Mines and Geology, Reno. Special Pub. No. 2.
- Howard, K. A., 1971. Paleozoic metasediments in the northern Ruby Mountains, Nevada. *Geological Society of America Bulletin, Miscellaneous Investigations*, Map 1-1136.
- Jackson, M.L. and Mackenzie, R. C., 1964. Chemical analysis in the quantitative mineralogical examination of clays. In: Cl. Rich and G.W. Kunze (Editors), *Soil Clay Mineralogy, A Symposium*. The University of North Carolina Press, Chapel Hill, pp. 313-325.
- Jenny, H., 1980. *The Soil Resource*. Springer-Verlag, New York, 377 pp.
- Jensen, M. E., Simonson, G. H., and Keane, R. E., 1989. Soil temperature and moisture regime relationships within some rangelands of the Great Basin. *Soil Sci.*, 147: 134-139.

- Kittrick, J. A., 1969. Soil minerals in the Al_2O_3 - SiO_2 - H_2O system and a theory of their formation. *Clays and Clay Minerals*, 17:157-167.
- Locke, W. W., 1979, Etching of Hornblende grains in arctic soils: an indicator of relative age and paleoclimate. *Quaternary Research*, 197-212.
- Machette, M. N., 1985. Calcic soils in the southwestern United States. p. 1-21. In: D.L. Weide, Editor, *Soils and Quaternary geology of the southwestern United States*. Geol. Soc. Am. Spec. Pap. 203.
- Mayer, L., 1986. The distribution of calcium carbonate in soils: A computer simulation using program CALSOIL. U.S. Geological Survey Open File Report 86-155.
- Mayer, L., McFadden, L. D., and Harden, J.W. 1988. Distribution of calcium carbonate in desert soils: a model. *Geology*, 16:303-306.
- McFadden L. D., and Hendricks, D. M., 1985. Changes in the content and composition of pedogenic iron oxyhydroxides in a chronosequence of soils in southern California. *Quaternary Research*, 23:189-204.
- McFadden, L.D. and Tinsley, J.C. 1985. Rate and depth of pedogenic-carbonate accumulation in soils: formation and testing of a compartment model. p. 23-42. In: D.L. Weide, Editor, *Soils and Quaternary geology of the southwestern United States*. Geol. Soc. Am. Spec. Pap. 203.
- McFadden, L. D., R.G. Amundson, and O.A. Chadwick. 1991. Numerical modeling, chemical, and isotopic studies of carbonate accumulation in soils of Arid Regions. pp. 17-35. IN: W.D. Nettleton, Editor, *Occurrence, Characteristics, and Genesis of Carbonate, Gypsum, and Silica Accumulations in Soils*. SSSA Special Paper No. 26.

- McFadden, L. D., Wells, S. G., and Jercinovich, M. J., 1987. influences of eolian and pedogenic processes on the origin and evolution of desert pavements. *Geology*, 15:504-508.
- Mears, B., Jr., 1981. Periglacial wedges and the late Pleistocene environment of Wyoming's intermountain basins. *Quaternary Research*, 15:171 -198.
- Mifflin, M. D., and Wheat, M. M., 1979. Pluvial Lakes and estimated pluvial climates of Nevada. Nevada Bureau of Mines and Geology Bulletin 94, University of Nevada, Reno, 57 pp.
- Morrison, R. B., 1991. Quaternary stratigraphic, hydrologic, and climatic history of the Great Basin, with emphasis on Lakes Lahontan, Bonneville and Tecopa. In: R.B. Morrison, Ed., Quaternary Nonglacial Geology: Conterminous United States. *The Geology of North America*, K-2, Geol. Soc. of Am., Boulder, CO., pp. 283-320.
- Nelson, R. E., and Nettleton, W. D., 1975. Some properties of smectite and mica in clays of soils in dry regions. *Geoderma*, 14:247-253.
- Nettleton, W. D., and Brasher, B. R., 1983. Correlation of clay minerals and properties of soils in the western United States. *Soil Sci. Soc. Am. J.*, 47:1032-1036.
- Nettleton, W. D., and Peterson, F. F., 1983. Aridisols. p. 165-215, In: L.P. Wilding, N.E. Smeck, and G.F. Hall, Editors, *Pedogenesis and Soil Taxonomy, II. The Soil Orders*. Developments in Soil Science 11 B, Elsevier, Amsterdam.
- Nikiforoff, C. C., 1953. Pedogenic criteria of climate changes. pp. 189 - 200. In: H. Shapley, Editor, *Climatic Change: Evidence, Causes and Effects*. Harvard University Press, Cambridge, Mass.

- Peterson, F. F., 1980. Holocene desert soil formation under sodium influence in a playa-margin environment. *Quaternary Research*, 13:172-186.
- Peterson, F. F., 1981. Landforms of the basin and range province defined for soil survey. Technical Bull. 28, Nevada A&S, Reno, Nevada, 52 pp.
- Porter, S.C. 1989. Some geological implications of average Quaternary glacial conditions. *Quaternary Research*, 32:245-261.
- Reheis, M. C., 1987. Climatic implications of alternating clay and carbonate formation in semi-arid soils of south-central Montana. *Quaternary Research* 27:270-282.
- Reheis, M. C., 1990. Influence of climate and eolian dust on the major-element chemistry and clay mineralogy of soils in the northern Bighorn Basin, U.S.A. *Catena* 17:219-248.
- Reheis, M. C., Harden, J. W., McFadden, L. D., and Shroba, R. R., 1989. Variation in rates of development and description of late Quaternary soils, Silver Lake playa, California. *Soil Sci. Soc. Am. J.* 53:1127-1140,
- Schmidlin, T. W., Peterson, F. F., and Gifford, R. O., 1983. Soil temperature regimes in Nevada. *Soil Sci. Soc. Am. J.* 47:977-982.
- Schwertmann, U, and Taylor, R. M., 1989. Iron oxides. pp. 379-438. In: J.B. Dixon and S.B. Weed, Editors, *Minerals in Soil Environments*, second edition. *Soil Sci. Soc. Am. Book Series No. 1.*
- Smith, G. I., and Street-Perrot, F. A., 1983. Pluvial lakes in the western United States. In: H.E. Wright, Editor, *The Late Pleistocene*, Vol 1, University of Minnesota Press, Minneapolis. pp. 190-212.

- Snyder, C. T., Hardman, D., and Zdenek, F. F., 1964. Pleistocene lakes in the Great Basin. U.S. Geological Survey, Misc. Geol. Invest. Map I-416.
- Stoops, G., and Jongerius A., 1975. Proposal for a micromorphological classification in soil materials. 1. A classification of the related distribution of fine and coarse particles. *Geoderma*, 13:189-200.
- Tan, K.H., 1992. *Principles of Soil Chemistry*. 2nd ed. Marcel Dekker, New York.
- Thompson, R. S., 1992. Late Quaternary environments in Ruby Valley, Nevada. *Quaternary Research*, 37:1-15.
- Thompson, R. S., and Mead, J. I., 1982. Late Quaternary environments and biogeography in the Great Basin. *Quaternary Research*, 17:39-55.
- Thorntwaite, C. W., 1948. Approach toward a rational classification of climate. *Geograph. Rev.*, 38:55-94.
- US-Weather Bureau, 30-year normal monthly precipitation-temperature-data-1931-1961-Card Deck 490, San Diego, CA.
- USDA-Soil Conservation Service, 1976, *National Range Handbook*. U.S. Govt. Printing Office, Wash., DC.
- USDA-Soil Conservation Service, 1984. *Procedures for collecting soil samples and methods for analysis for soil survey*. U.S. Govt. Printing Office, Wash., DC,
- USDA-Soil Conservation Service, 1992. *Soil survey laboratory methods and procedures for collecting soil samples*. U.S. Govt. Printing Office, Wash., DC.
- USDA-Soil Conservation Staff, 1951. *Soil survey manual*. U.S. Dept. Agricul. Handbook 18. U.S. Govt. Printing Office, Wash., DC.

Wayne, W. J., 1984. Glacial chronology of the Ruby Mountains-East Humbolt Range, Nevada. *Quaternary Research*, 21:286-303.

Wells, S. G., McFadden, L. D., and Dohernwend, J. C., 1987. Influence of late Quaternary climatic changes on geomorphic and pedogenic processes on a desert piedmont, eastern Mojave Desert, California. *Quaternary Research* 27: 130-146.

FIGURES

Figure 1. Map of northern Great Basin showing the approximate extent of latest Pleistocene lakes, their modern-day remnants, and the Ruby Mountain study area (modified from Snyder et al., 1964).

Figure 2. Perspective view from the northwest showing the Ruby mountains, Lamoille Canyon, and the sample sites.

Figure 3. Relationships among organic carbon, exchange acidity, base saturation, and effective moisture along the transect. Values are integrated for the top 1 m of the soils, normalized by water retention difference (WRD) to eliminate soil texture bias, and plotted against effective moisture.

Figure 4. Plain polarized light photomicrographs of the soil profile at site 2 showing: A) silans (s) overlying illuviation argillans (1) along voids (v) in the 2C horizon; and B) the swelling induced skeletal-massive fabric in the smectite rich Bt2 horizon.

Figure 5. Paired plain-polarized and cross-polarized light photomicrographs of the 2Bqkm horizon from the soil profile at site 2. This horizon is the site of maximum accumulation of opaline silica and carbonate due to limited leaching depth. The micrographs show: A & B) fine sand- and silt-size nodules and concretions of opaline silica and carbonate at the upper horizon boundary, and C & D) repeating layers of opaline silica (o) and carbonate (k).

Figure 6. Relative quantity of X-ray identified minerals in the clay-size fraction from B horizons of soil profiles based on interpretation of peak heights.

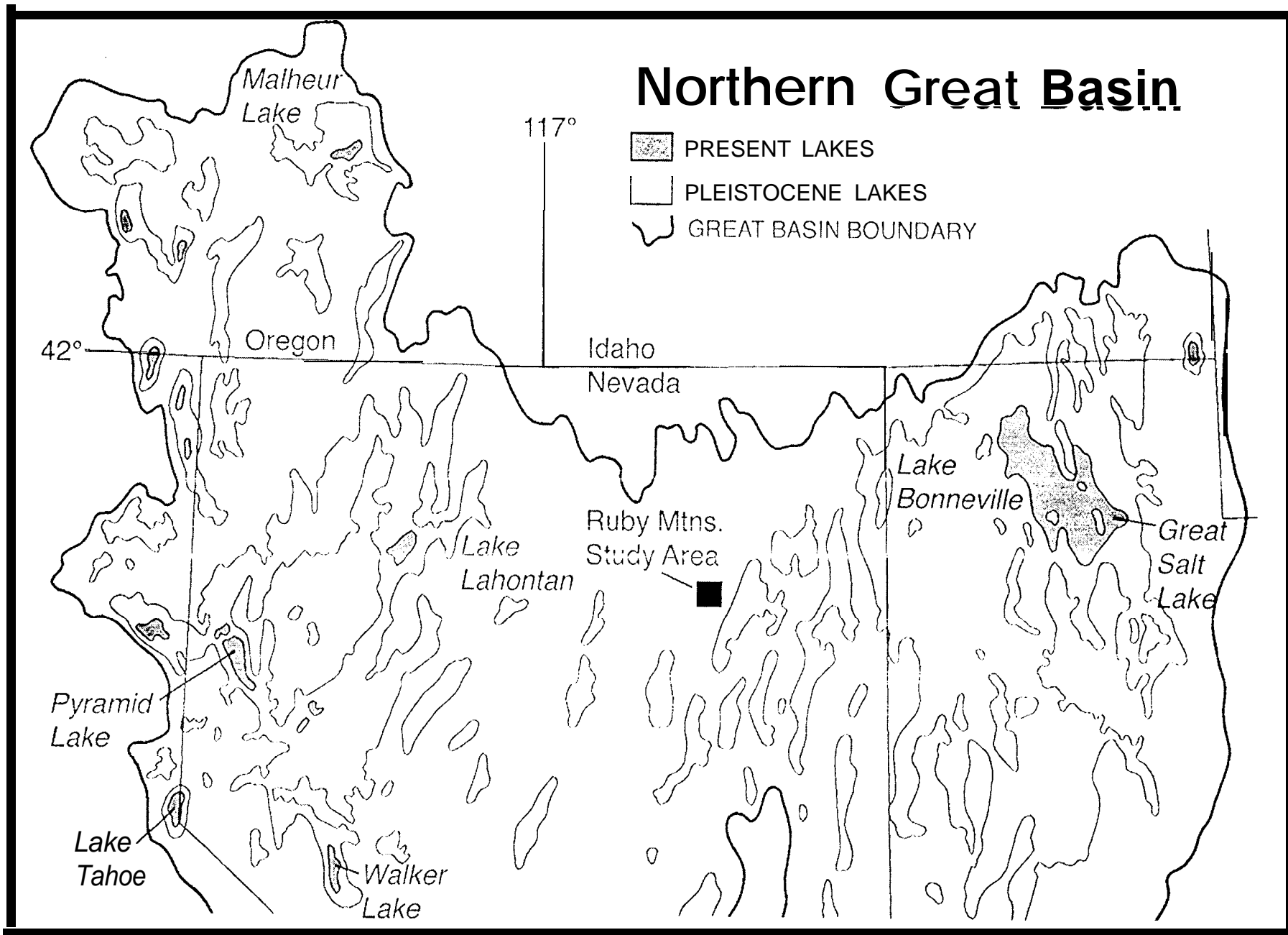
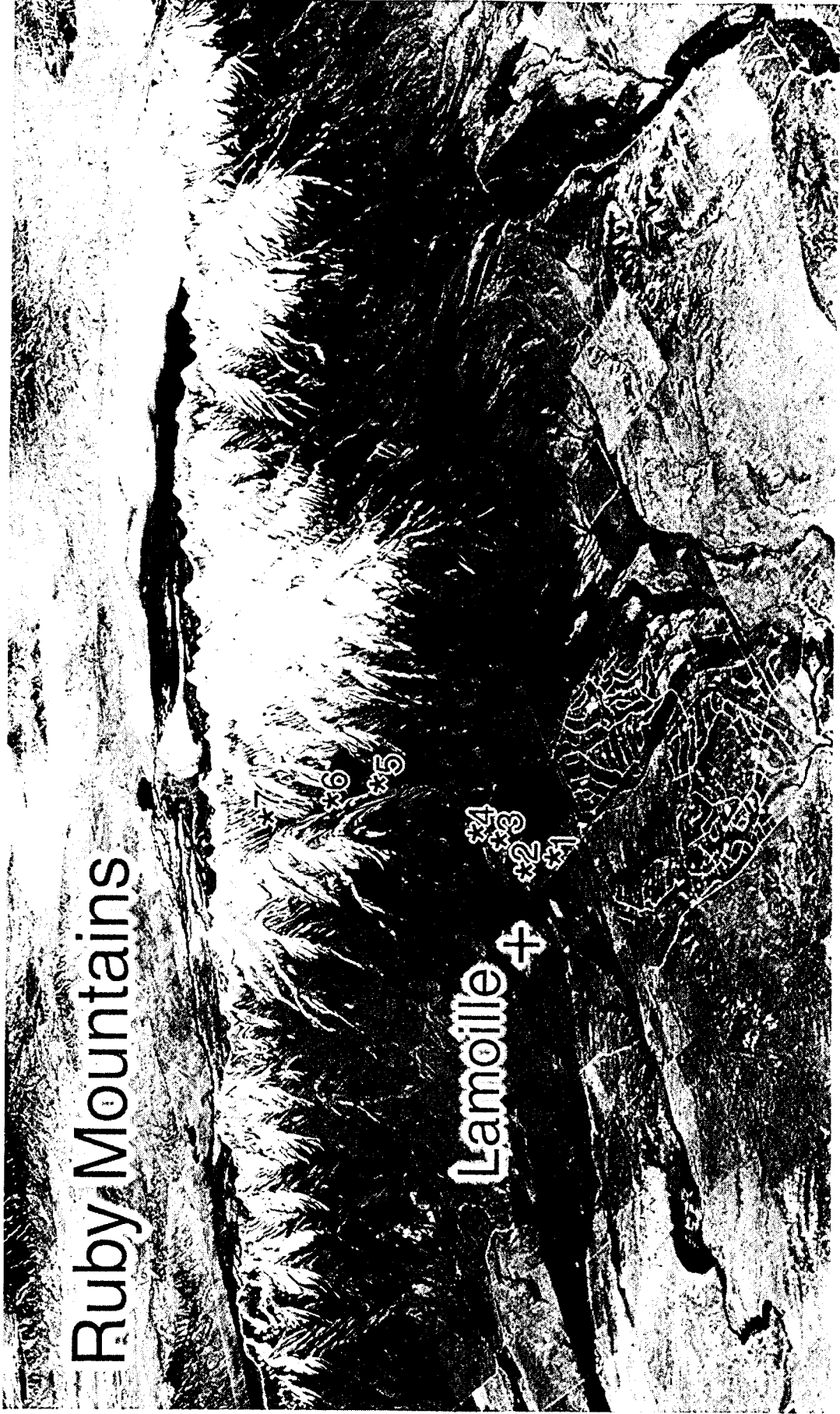


Fig 1



Ruby Mountains

Lamoille +

#6
#5
#4
#3
#2
#1

Fig 2

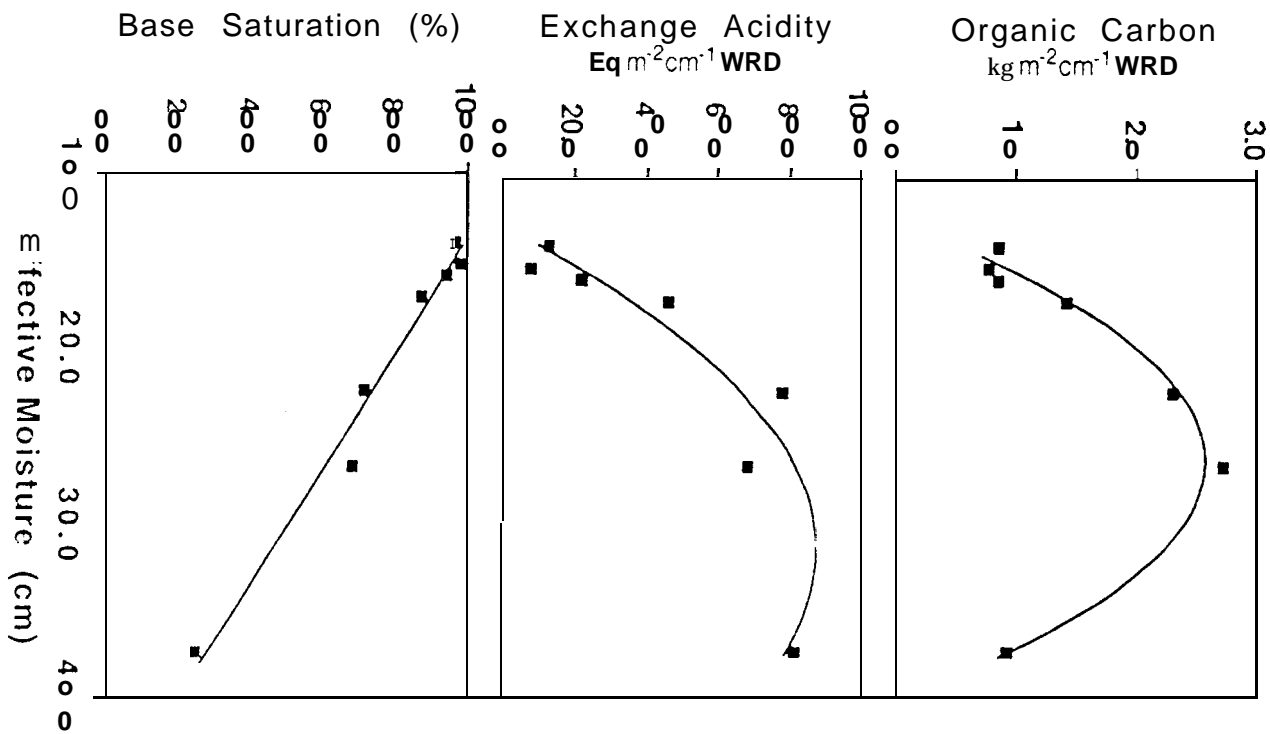


Fig 3

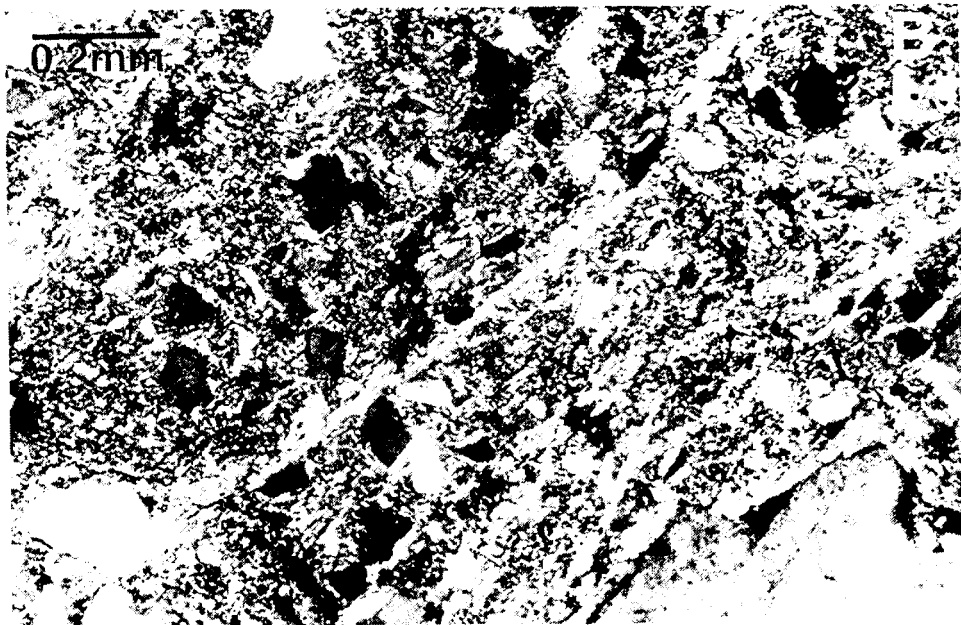
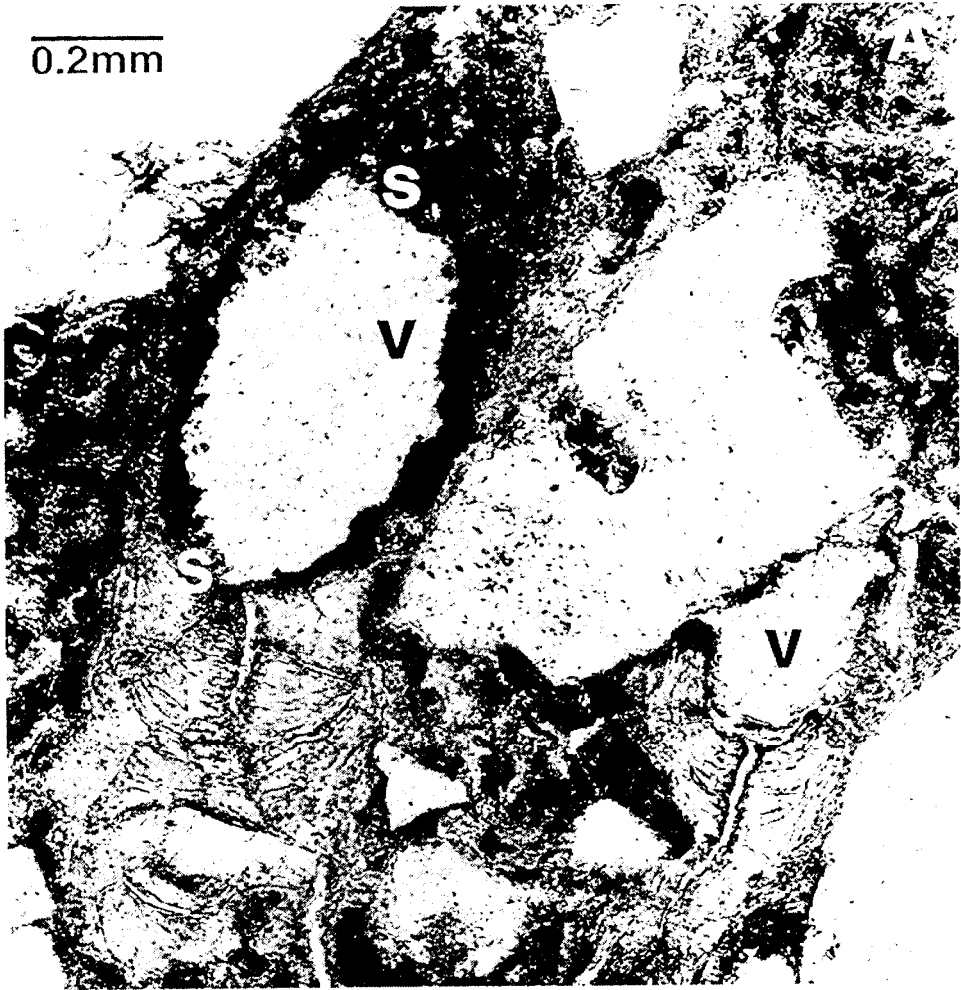


Fig 4

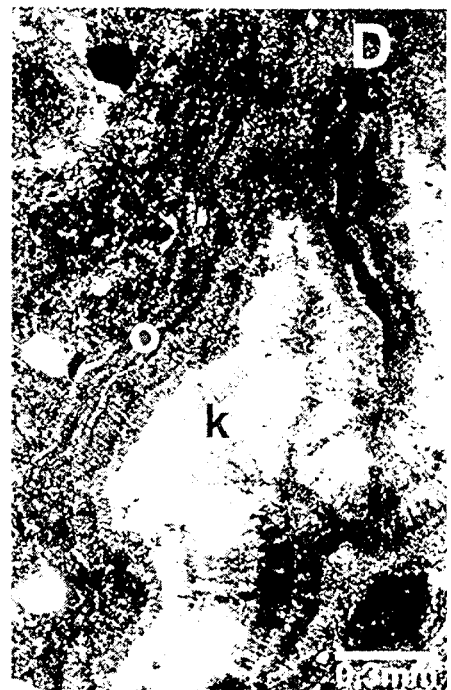
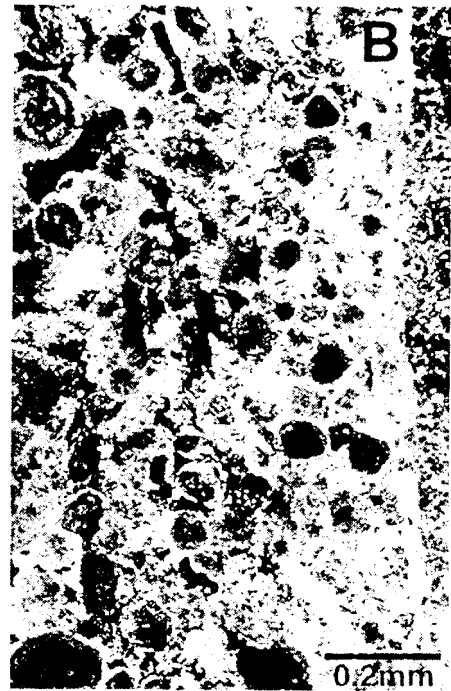
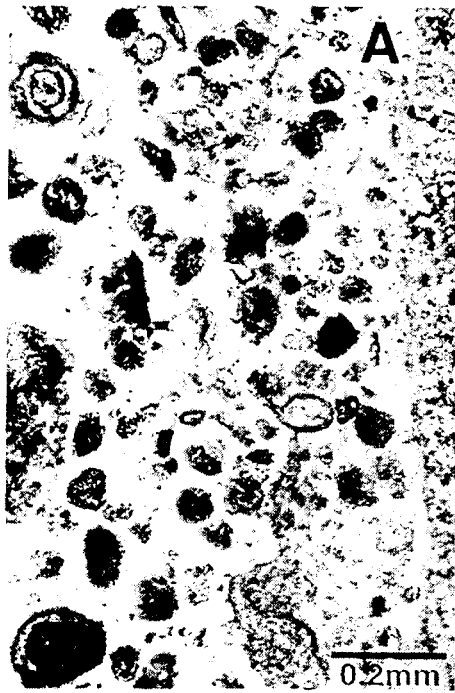


Fig 5

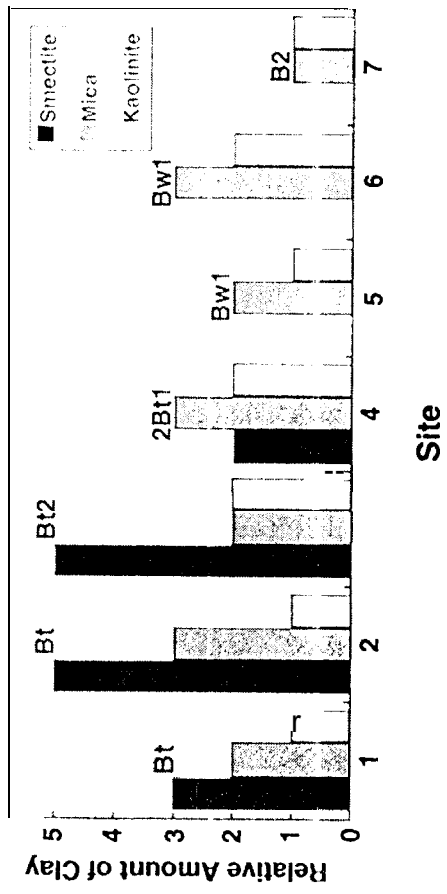


Fig 6

Table 1: Physiography and biomass production of the study sites.

Site	Location	Soil Landscape *	Slope & Aspect	Biomass Production ++ *	Vegetation +++
				kg ha ⁻¹ yr ⁻¹	
1	366 m W. & 26 m S. of the NE. cor. Sec. 27 T. 33 N., R. 57 E.	Summit of alluvial piedmont remnant	3%; SW	500	<u>Artemisia tridentata wyomingensis</u> (15%), <u>Chrysothamnus viscidiflorus</u> (10%), <u>Sitanion</u> & (20%), <u>Elymus cinereus</u> (5%)
2	183 m W. & 152 m S. of the NE. cor. Sec. 25 T. 33 N., R. 57 E.	Summit of alluvial piedmont remnant	2%; N-NE	1,000	<u>Agropyron cristatum</u> (92%), <u>Sitanion hystrix</u> (tr), <u>Poa secunda</u> (3%), <u>Elymus cinereus</u> (5%)
3	46 m W. & 8 m N. of the SW. cor. Sec. 30 T. 33 N., R. 58 E.	Summit of Lamoille end moraine	3%; SE	600	<u>Poa secunda</u> (10%), <u>Artemisia tridentata wyomingensis</u> (43%), <u>Chrysothamnus viscidiflorus</u> (15%)
4	976 m. W. & 549 m N. of the SE. cor. Sec. 31 T. 33 N., R. 58 E.	Summit of Lamoille end moraine	3%; Ssw	700	<u>Agropyron spicatum</u> (19%), <u>Artemisia arbuscula</u> (16%), <u>Sitanion hystrix</u> (8%), <u>Poa secunda</u> (8%)
5	808 m E. & 244 m S. of the NW. cor. Sec. 16 T. 32 N., R. 58 E.	Summit of Angel Lake end moraine	2%; N	900	<u>Festuca idahoensis</u> (40%), <u>Agropyron spicatum</u> (20%), <u>Artemisia vaseyana</u> (29%), <u>Cercocarpus ledifolius</u> (8%), <u>Stipa occidentalis nelsonii</u> (10%)
6	671 m W. & 244 m S. of the NE. cor. Sec. 16 T. 32 N., R. 58 E.	Summit of Angel Lake lateral moraine	5%; NE	1,600	<u>Artemisia vaseyana</u> (26%), <u>Agropyron spicatum</u> (16%), <u>Stipa occidentalis nelsonii</u> (8%), <u>Elymus cinereus</u> (8%), <u>Poa nevadaensis</u> (8%)
7	1555 m E. & 610 m S. of the NE. cor. Sec. 31 T. 32 N., R. 59 E.	Summit of Angel Lake recessional moraine	3%; SW	1200	<u>Festuca idahoensis</u> (30%), <u>Populus tremuloides</u> (2%), <u>Stipa lettermanii</u> (30%), <u>Lromucarinat</u> (13%)

+ Terminology follows Peterson (1981) and Wayne (1984).

++ Estimated dry weight production of the present vegetation for all species at the site.

+++ Numbers in parenthesis are % of composition by dry weight of the dominant plant species present at the site.

‡ Procedures used to determine biomass production, dry weight basis, are outlined in the National Range Handbook, (USDA-Soil Conservation Service, 1976).

Table 2. Measured and calculated climatic and leaching data.

<u>Site</u>	<u>Elevation</u> (m)	<u>MAP</u> ⁺ (cm)	<u>MAAT</u> * (°C)	<u>Effective</u> <u>Moisture</u> ⁺⁺ (cm yr ⁻¹)	<u>MAST</u> ⁺⁺⁺ (°C)	<u>Calculated Depth</u> <u>of Leaching</u> (cm)
1	1770	30.9	7.7	14.0	9.3	100
2	1804	32.4	7.6	15.2	9.1	125
3	1853	34.3	7.3	15.9	8.9	200
4	1915	36.8	7.0	17.2	8.6	325
5	2134	45.6	4.5 ⁺⁺	22.4	6.3 ⁺⁺	550
6	2257	50.4	4.0	26.7	5.9	400
7	2637	65.7	3.4	37.4	4.7	650

+ Mean annual precipitation was calculated using a regression equation developed by USDI - BLM (Nevada State Office, Personal Communication) as follows:
 $MAI' \text{ (in.)} = 0.0048 - 15.66605 \text{ (ELEVATION, ft.)}; r = 0.92.$

* Mean annual air temperature was calculated based on a lapse rate of 0.5°C/ 100 m (Mifflin and Wheat, 1979; Schmedlin et al., 1983). The initial datum selected for calculation was 7.0 °C at the Lamoille weather station (US Weather Bureau, Card Deck 490).

++ The calculated data were modified to reflect topographic relationships that enhanced cold air drainage from higher altitudes.

-t++ Mean annual soil temperatures were calculated using regression equations developed by Jensen et al., (1983) as follows: Sites 1-4, $MAST \text{ (°C)} = 18.70 - 0.0053 \text{ (Elevation, m)}$; sites 5-7, $MAST \text{ (°C)} = 13.12 - .0032 \text{ (Elevation, m)}$.

Table 3. Physical properties affecting water retention.

<u>Horizon</u>	<u>Depth</u>	Coarse Frgs >2 mm	Sand 2-.05	Silt .05-.002	Clay <.002	Total Porosity	H ₂ O at at 1.5 MPa	H ₂ O at Field Capacity	Water Retention Difference	Cumulative Water at Field Capacity
	cm	-----% by volume -----					-----g kg ⁻¹ -----		cm cm ⁻¹	cm
Site 1, fine, montmorillonitic, mesic Xerollic Durargid										
A1	0-18	5	17	16	10	52	140	287	.15	2.70
A2	18-40	3	18	20	10	49	130	285	.16	6.22
Bt	40-63	2	14	9	23	52	282	400	.12	8.98
2Btk	63-85	19	15	10	19	37	226	329	.12	11.18
2Bqkm	85-90	8	26	19	10	37	99	233	.13	11.83
Site 2, fine, montmorillonitic, mesic Typic Durixeroll										
Al	0-11	1	10	23	14	53	180	322	.14	1.56
A2	11-23	1	12	25	14	48	173	327	.15	3.36
A3	23-40	1	13	27	12	47	158	320	.16	6.08
Bt	40-62	2	9	18	20	51	237	381	.14	9.16
Bk	62-95	2	12	19	21	46	242	369	.13	13.45
2Bqkm	95-125	49	28	3	3	17	22	99 ⁺	.08	15.85
Site 3, fine, montmorillonitic, mesic Xerollic Haplargid										
Al	0-6	18	19	17	8	38	103	230 ⁺	.13	.78
A2	6-20	14	19	16	10	41	129	255 ⁺	.13	2.60
Bt1	20-38	19	21	11	11	38	153	259 ⁺	.11	4.58
Bt2	38-62	27	17	4	14	38	201	270 ⁺	.07	6.26
BC3	62-86	33	15	4	13	36	211	259 ⁺	.05	7.46
Bk	86-150	49	17	9	6	19	83	151 ⁺	.08	12.58
c	150-200	50	21	6	6	17	64	122 ⁺	.06	15.58

Table 3. Physical properties affecting water retention (continued)

<u>Horizon</u>	<u>Depth</u>	<u>Coarse Frag</u> <u>>2 mm</u>	<u>Sand</u> <u>2 - .05</u>	<u>Silt</u> <u>.05 - .002</u>	<u>Clay</u> <u><.002</u>	<u>Total Porosity</u>	<u>H₂O at</u> <u>at 1.5 MPa</u>	<u>H₂O at</u> <u>Field Capacity</u>	<u>Water Retention Difference</u>	<u>Cumulative Water at Field Capacity</u>
	cm	-----% by volume -----					-----g kg ⁻¹ -----		cm cm ⁻¹	cm
Site 4, loamy-skeletal, mixed, mesic Xerollic Haplargid										
Al	0-8	34	22	10	5	29	62	151	.09	.72
ABt	8-20	34	18	11	8	29	95	186	.09	1.80
2Bt1	20-43	52	15	4	8	21	91	143	.05	2.95
2Bt2	43-66	46	24	5	6	19	62	120	.06	4.33
2BCt	66-84	80	10	2	2	6	18	43	.03	4.87
2C1	84-104	55	19	10	3	13	29	98	.07	6.27
2C2	104-114	63	23	3	2	9	12	5	.05	6.77
Site 5, loamy-skeletal, mixed, Typic Cryoboroll										
Al	0-11	52	13	7	4	24	58	127	.07	.77
A2	11-20	72	9	4	2	13	32	70	.04	1.13
Bw	20-28	55	21	6	3	15	31	95	.06	1.73
C1	28-60	75	13	3	1	8	10	47	.04	2.93
C2	60-100	73	16	3	1	7	09	48	.04	4.53
Site 6, loamy-skeletal, mixed, Typic Cryoboroll										
Al	0-10	34	17	6	2	41	53	182	.13	1.33
A2	10-20	36	18	7	4	35	65	190	.13	2.60
A3	20-28	42	22	7	5	24	62	168	.11	3.48
Bw1	28-41	50	21	7	3	19	40	123	.08	4.52
Bw2	41-61	48	25	4	2	21	24	89	.07	5.92
c1	61-91	53	25	4	2	16	17	73	.06	7.72

Table 3. Physical properties affecting water retention (continued).

<u>Horizon</u>	<u>Depth</u>	Coarse Frag >2 mm	Sand 2 - .05	Silt .05 - .002	Clay <.002	Total Porosity	H ₂ O at at 1.5 MPa	H ₂ O at Field Capacity	Water Retention Difference	Cumulative Water at Field Capacity
	cm	-----% by volume -----					-----g kg ⁻¹ -----		cm cm ⁻¹	cm
Site 7, loamy-skeletal, mixed, Typic Cryumbrept										
A1	0-7	3	13	12	7	65	122	274	.15	1.05
A2	7-16	5	18	17	8	52	120	262	.14	2.31
Bw	16-42	12	19	18	7	44	98	235	.14	5.95
C1	42-64	37	26	10	2	25	26	134	.11	8.37
C2	64-200	72	17	2	1	8	07	45	.04	13.81

+10 kPa

Table 4. Selected chemical properties for the <2 mm fraction and K₂O content of the <2 μm clays.

<u>Horizon</u>	<u>Depth</u> cm	<u>Organic Carbon</u> (%)	<u>Exchange Acidity</u> (meq 100g ⁻¹)	<u>Base Saturation</u> (% by sum of M ⁺)	<u><2 mm CaCO₃</u> g kg ⁻¹	<u>pH</u>	<u>Exchangeable Ca P e r t _</u> (%)	<u>K₂O in <? μm Clay</u> g kg ⁻¹
Site 1, fine, montmorillonitic, mesic Xerollic Durargid								
A1	0-18	1.70	0.5	99	tr	7.5	ND ⁺	0
A2	18-40	0.70	1.6	92	--	7.2	89 (73)*	ND
Bt	40-63	0.55	3.2	93	--	6.9	84 (69)	ND
2Btk	63-85	0.52	0	100	190	7.6	ND	ND
2Bqkm	85-90+	0.27	0	100	150	7.7	ND	ND
Site 2, fine, montmorillonitic, mesic Typic Durixeroll								
A1	0-11	2.84	1.2	97	tr	7.4	ND	ND
A2	11-23	1.00	1.1	97	tr	7.3	ND	ND
A3	23-40	0.78	1.5	95	tr	7.3	ND	11
Bt	40-62	0.48	1.1	98	tr	7.7	ND	ND
Bk	62-95	0.54	0	100	300	7.6	ND	ND
2Bqkm	95-125	0.37	0	100	340	7.6	ND	ND
2C	125-425	0.06	1.5	93	tr	7.2	ND	ND
Site 3, fine, montmorillonitic, mesic Xerollic Haplargid								
A1	0-6	1.33	1.0	95	tr	7.5	ND	11
A2	6-20	1.49	2.5	87	tr	6.7	ND	ND
Bt1	20-38	0.48	2.6	87	tr	6.5	ND	14
Bt2	38-62	0.41	1.7	95	tr	7.3	ND	ND
BC3	62-86	0.17	0.3	99	tr	8.0	ND	ND
Bk	86-150	0.14	0.2	100	60	8.0	ND	ND
c	150-200	0.08	0.1	100	tr	7.6	ND	7

Table 4. Selected chemical properties for the <2 mm fraction and K₂O content of the <2 μm clays (continued).

<u>Horizon</u>	<u>Depth</u>	<u>Organic Carbon</u>	<u>Exchange Acidity</u>	<u>Base Saturation</u>	<u><2 mm CaCO₃</u>	<u>pH</u>	<u>Exchangeable Ca Percentage</u>	<u>K₂O in <2 μm Clay</u>
	cm	(%)	(meq 100g ⁻¹)	(% by sum of M+)	g kg ⁻¹		(%)	g kg ⁻¹
Site 4, loamy-skeletal, mixed, mesic Xerollic Haplargid								
A1	0-8	1.44	1.7	85	--	6.4	80 (63)	25
ABt	8-20	1.26	2.7	84	--	6.4	80 (62)	ND*
2Bt1	20-43	0.67	2.7	86	--	6.5	77 (61)	25
2Bt2	43-66	0.27	1.9	85	--	6.4	76 (60)	ND
2BCt	66-84	0.26	0.8	91	--	6.3	76 (65)	27
2C1	84-104	0.14	0.6	89	--	6.2	79 (65)	ND
2C2	104-114	0.17	0	100	--	6.2	76 (72)	25
Site 5, loamy-skeletal, mixed, Typic Cryoboroll								
A1	0-11	3.14	6.3	77	--	6.1	86 (66)	ND
A2	11-20	1.46	4.2	77	--	6.1	85 (66)	ND
Bw	20-28	0.70	2.5	73	--	5.9	78 (60)	ND
C1	28-60	0.30	1.4	74	--	5.9	77 (57)	ND
C2	60-100	0.16	1.2	67	--	5.4	68 (53)	ND
Site 6, loamy-skeletal, mixed, Typic Cryoboroll								
A1	0-10	8.50	14.4	67	--	5.6	76 (58)	20
A2	10-20	4.20	8.4	71	--	5.9	84 (61)	ND
A3	20-28	2.75	6.6	69	--	5.8	78 (58)	ND
Bw1	28-41	0.96	3.5	67	--	5.8	79 (53)	21
Bw2	41-61	0.51	2.2	69	--	5.7	71 (52)	ND
c1	61-81	0.27	1.7	67	--	5.7	81 (51)	ND
C2	81-91	0.19	0.9	69	--	5.7	67 (48)	19

Table 4. Selected chemical properties for the <2 mm fraction and K₂O content of the <2 μm clays (continued)

<u>Horizon</u>	<u>Depth</u>	<u>Organic Carbon</u>	<u>Exchange Acidity</u>	<u>Base Saturation</u>	<u><2 mm CaCO₃</u>	<u>pH</u>	<u>Exchangeable Ca Percentage</u>	<u>K₂O in <2 μm Clay</u>
	cm	(%)	(meq 100g ⁻¹)	(% by sum of M+)	g kg ⁻¹		(%)	g kg ⁻¹
Site 7, loamy-skeletal, mixed, Typic Cryumbrept								
A1	0-7	6.31	18.5	62	--	---	71 (54)	ND
A2	7-16	2.30	14.9	40	--	5.0	42 (30)	ND
Bw	16-42	1.49	15.4	29	--	4.9	34 (22)	ND
C1	42-64	0.31	5.4	14	--	5.1	18(10)	ND
C2	64-200	0.26	3.8	19	--	5.2	22 (15)	ND

* Because of the presence of carbonate, exchangeable Ca was not determined (ND) for these samples.

‡ Exchangeable Ca was calculated in two ways. First it is reported as the percentage of the NH₄OAc exchange capacity. Also, it is reported in parentheses as the percentage of bases + exchange acidity.

Table 5. Micromorphological description of selected horizons.

Horizon & Depth (cm)	Related+ Distribution Pattern	Plasmic‡ Fabric	C o m m e n t s
Site 1, fine, montmorillonitic, mesic Typic Durargid			
A1 0-18 R2346	single-space porphyric (porphyric)	silasepic	The sand grains consist of quartz (50-70%), k-feldspar (15-20%), biotite and muscovite (10%), and some plagioclase, hornblende, pyroxene, calcite, zircon, and a few volcanic glass shards. There are thin illuviation argillans around most sand grains. The glass shards and biotite are partly weathered; the latter have expanded on their ends. Some of the plagioclase grains, have weathering pits and the hornblende and pyroxene are weathered along cleavage traces.
Bt 40-63 R2347	double-space porphyric (porphyric)	skel-masepic	There are many shrinkage cracks but no illuviation argillans.
2Bqkm 85-90 R2348	single-space porphyric (porphyric)	skelsepic	Embedded grain argillans coated in turn with silans or calcans are common. The bottoms of many of the grains have 0.1 mm thick coatings of opaline silica. There are abundant fine sand-size opaline silica nodules and calcite is dispersed throughout the matrix.
Site 2, fine, montmorillonitic, mesic Typic Durixeroll			
A2 11-23 R2332	single-space porphyric (porphyric)	silasepic-skelsepic	Skeleton grains have thin illuviation argillans and are composed of the same kind and amount as those at site one. There are a few volcanic glass shards as well. Biotite is the most weathered with the ends of the grains expanded losing pleochroism. Hornblende and pyroxene have weathered along cleavage traces. To a lesser extent feldspars are also weathered along cleavages and the sericite inclusions. Quartz and muscovite are unweathered.
Bt 40-62 R2333	double-space porphyric (porphyric)	skel-masepic	There are many desiccation cracks but no illuviation argillans.

Table 5. Micromorphological description of selected horizons (continued).

Horizon & Depth (cm)	Related+ Distribution Pattern	Plasmic [‡] Fabric	Comments
2Bqkm 95-125 R2334	open porphyric	crystic-isotc	The laminar dunpan consists of repeating layers of opaline silica nodules and concretions (0.1 -0.3 mm in diameter) in a mass of silt-size calcite interspersed with massive layers of opal, calcite, and oriented clays. Calcite fills cracks within the duripan. Opaline silica is clear in plane light and isotropic under crossed polarized light. Its index of refraction is less than the impregnating medium. There are many layers of opal-CT or chalcedony (10-30 μm thick) within thicker layers of oriented clays.
2C 125-425 R2335	single-space porphyric (porphyric)	skelsepic-isotc	Embedded grain argillans are common. Void and channel illuviation argillans and silans are common. The silans are silt-sized nodules of opaline silica cemented along the walls of voids. They may be either dense or porous. Opaline silica also partly impregnates the argillans, destroying part of their orientation.
Site 3, Fine, montmorillonitic, mesic Xerollic Haplargid			
A2 6-20 R2336	single-space porphyric (porphyric)	silasepic	The skeleton grains are coated with thin illuviation argillans and are composed of the same kind and amount of minerals noted for site one except that there are more glass shards. The biotite is mostly weathered, the pyroxene and hornblende are somewhat weathered while feldspar and muscovite are unweathered.
Bt2 38-62 R2337	single-space porphyric (porphyric)	masepic	There are many shrinkage cracks but no illuviation argillans. Some of the muscovite is weathered along the ends of the grains.
Bk 86-150 R2338	single-space porphyric (porphyric)	masepic	Common shrinkage cracks. A few areas have less clay and thin illuviation argillans in voids and channels.
c 150+ R2339	single-space porphyric (porphyric)	ma-mosepic	Some primary calcite. Calcans are common on the under sides of gravel and in a few voids and channels but there are no illuviation argillans.

Table 5. Micromorphological description of selected horizons (continued).

Horizon & Depth (cm)	Related+ Distribution Pattern	Plasmic* Fabric	Comments
Site 4, Loamy-skeletal, mixed, mesic Xerollic Haplargid			
Al 0-3 R2349	enaulic (granoidic)	skelsepic	Silt and sand aggregates only partly fill the voids between the skeleton of coarse particles. Many of the sand grains have thin argillans, others have silt coatings. Skeleton grains have fine fractures mostly along mineral boundaries. These are lined with argillans. Most of the aggregates are of silts and sands without clay bridging. Biotite grains are frayed on edges and some layers have weathered to clay.
Bt1 20-43 R2350	chitonic (granoidic)	skelsepic	Silt and sand aggregates <i>only</i> partly fill the voids between the skeleton of coarse particles. These aggregates are bonded by clay bridges. Argillans are on skeleton grains also. Biotite has frayed edges, some biotite has exfoliated. Plagioclase is weathered along cleavage traces.
Bt2 43-66 R2351	chitonic (granoidic)	skelsepic	Silt and sand aggregates only partly fill the voids between the skeleton of coarse particles. These aggregates are bonded by clay bridges. Argillans are on skeleton grains also. Biotite has frayed ends, some biotite has exfoliated. Plagioclase and sericitized feldspar are weathered. Many of the larger grains of quartz and feldspar have a craze cracking pattern. Similar features occur in upper horizons also and may result from Pressure and movement of the glacier.
Site 5, Loamy-skeletal, mixed Typic Cryoboroll			
Al 0-11 R2343	enaulic (matrigranic)	silasepic	Cutans of organic matter, silt, and clay coat sand grains composed of quartz (50-70%), K-feldspar (15-20%), biotite and muscovite (10%), and some plagioclase, hornblende, pyroxene, and zircon among other minerals. Ends of the biotite are strongly weathered and partly expanded. Kaolinite is the apparent weathering product. Augite is weathered to brown clay along cleavage traces but feldspar and muscovite are unweathered.

Table 5. Micromorphological description of selected horizons (continued).

Horizon & Depth (cm)	Related+ Distribution Pattern	Plasmic* Fabric	Comments
Bw 20-30 R2344	close porphyric (porphyric)	silasepic	Weathering is similar to that in A1. There is abundant fine sand and silt size muscovite. There are no illuviation argillans in voids or channels but there are a few thin free grain argillans.
c I 30-60 R2345	close porphyric (porphyric)	silasepic	Weathering is similar to that in the A1. There are no illuviation argillans.
Site 6, Loamy-skeletal, mixed Typic Cryboroll			
A1 0-10	chitonic (chlamydic)	skelsepic	Many of the skeleton grains have very thin illuviation argillans. Feldspars are fresh, most are orthoclase. Biotites have frayed ends. Decaying roots and organic debris dominate the section. There are not enough silts and clays to fill the voids between the skeleton grains.
Bw1 28-41	chitonic (chlamydic) ^f	skelsepic	Some cutans on grains are mixtures of silt and clay, others are clays and well oriented. Biotites have frayed ends and a few have layers that have weathered to clay. There are not enough silts and clays to fill the voids between skeleton grains. There are some aggregates of silt and clay. These grains are held together by clay bridges.
Site 7, Loamy-skeletal, mixed Pachic Cryboroll			
A2 7-16 R2340	close porphyric (junctional porphyric)	silasepic	Many of the skeleton grains have cutans of mixtures of clay, silt and organic matter. Feldspars are mostly unweathered; biotite grains are weathered on the ends, some are expanding and bent. Weathering product apparently is kaolinite. Pyroxenes and hornblende are slightly weathered along cleavage traces. There are some glass shards.

Table 5. Micromorphological description of selected horizons (continued).

Horizon & Depth (cm)	Related + Distribution Pattern	Plasmic [‡] Fabric	Comments
Bw 16-42 R2341	single-space porphyric (iunctic porphyric)	silasepic	A few of the skeleton grains have illuviation argillans; most have cutans of clay, silt and organic matter. Weathering is similar to that of the A2 horizon. There are some glass shards.
c I 42-64 R2342	close porphyric (iunctic porphyric)	silasepic	Most of the skeleton grains have cutans and bridges of silt and clay. Orientation of most of the clay is weak. There are very few illuviation void argillans with moderate orientation. Skeleton grains are cracked extensively but weathering is minimal.

[†]The terminology is that of Stoops and Jongerius (1975) and of Brewer (1976), in parentheses.

[‡]The terminology is that of Brewer (1976).

Table 6. Desert loess addition and rates of clay formation for selected sites.

Site	Desert Loess Additions [†]			Rates of Desert Loess Additions [†]			Clay Formation ⁺⁺	
	Silt kg cm-z	Clay kg cm-z	Silt + Clay kg cm-z	Silt g cm-z kyr ⁻¹	Clay g cm-z kyr ⁻¹	Silt + Clay g cm-z kyr ⁻¹	Amounts kg cm-z	Rates g cm-z kyr ⁻¹
3	0.6	2.7	3.3	0.004	0.02	.02	2.0	0.01
5	0.4	0.3	0.7	0.02	0.02	.04	0.15	0.01
6	0.2	0.5	0.7	0.01	0.03	.04	0.35	0.02

[†]Additions to the sola of the soils are calculated on a whole soil basis and are sums of A and B horizon volumes of silt or clay multiplied by 2.65 g cm⁻³, after correcting for silt or clay in the C horizon.

[†]Rates of silt, clay, and silt + clay additions were derived by dividing the amounts in the sola by either 18 kyr in the case of sites 5 and 6 or by 150 kyr in the case of site 3.

⁺⁺To obtain the amount of clay formed, silt+ clay was reduced by a factor of 0.222 to account for the clay estimated to have arrived in the loess. The rate of clay formation for site 3 was calculated by dividing the clay formed by 150 kyr, and sites 5 and 6 by 18 kyr, the estimated ages of the materials and geomorphic surfaces.